Journal of Solid State Chemistry **147,** 592–600 (1999)
Article ID jssc.1999.8422, available online at http://www.idealibrary.com on IDEAL®

Synthesis and Structural Analysis of $Bi_{0.5}La_{13.5}Ti_8S_{29}Cl_4O_4$ and $La_{23.1}Ti_{16.2}S_{49}Cl_8O_8$: Two New Oxychlorosulfide Compounds with $^2_\infty[(Ti_4Q_2O_4)(TiQ_6)_{4/2}]$ Layers Where Q = S/Cl

Louis J. Tranchitella, James C. Fettinger, and Bryan W. Eichhorn

Department of Chemistry and Biochemistry, Center for Superconductivity Research, University of Maryland, College Park, Maryland 20742

Received March 17, 1999; in revised form May 24, 1999; accepted May 27, 1999

Two new titanium oxychlorosulfide compounds, $Bi_{0.5}La_{13.5}Ti_8S_{29}Cl_4O_4$ and $La_{23.1}Ti_{16.2}S_{49}Cl_8O_8$, were prepared from the elements and binaries (oxides and sulfides) at 950°C in evacuated quartz tubes in the presence of $LaCl_3$ flux. The compositions of the compounds were determined by wavelength dispersive X-ray analysis and single crystal X-ray diffraction. Both compounds have $^2_\infty[(Ti_4Q_2O_4)(TiQ_6)_{4/2}]$ oxysulfide layers (OS) that are separated by oxide-free Ti–Q layers (Q = S, Cl solid solution). For $Bi_{0.5}La_{13.5}Ti_8S_{29}Cl_4O_4$, the oxysulfide layers are separated by $[La_6Ti_2Q_{19}]$ layers containing isolated, distorted TiQ_6 octahedra. $La_{23.1}Ti_{16.2}S_{49}Cl_8O_8$ has $[La_{4.1}Ti_{4.9}Q_{20}]$ (A) and $[La_6Ti_{2.19}Q_{19}]$ (B) layers that alternatively stack with the oxysulfide layers along the c-axis following the sequence −A−OS−B−OS−A−OS−B−. The chloride ions could not be crystallographically differentiated from the sulfide ions. Crystal data for $Bi_{0.5}La_{13.5}Ti_8S_{29}Cl_4O_4$: orthorhombic, $Cmcm$, a = 14.7463(9) Å, b = 14.9009(8) Å, c = 22.680(4) Å, V = 4983.5(10) Å^3, Z = 4, T = 153(2) K, $R1(F)$ = 4.17%, $wR2(F^2)$ = 8.80% for all 2352 unique reflections. For $La_{23.1}Ti_{16.2}S_{49}Cl_8O_8$: monoclinic, $C2/m$, a = 14.8278(4) Å, b = 14.7241(3) Å, c = 20.2724(6) Å, β = 103.54(1)°, V = 4302.9(2)Å^3, Z = 2, T = 153(2), $R1(F)$ = 4.94%, $wR2(F^2)$ = 12.00% for all 3952 unique reflections. © 1999 Academic Press

INTRODUCTION

The synthesis and characterization of new transition metal oxysulfides has recently received a great deal of attention (1–10). The mixture of O^{2-} and S^{2-} ions in the crystal lattice has been shown to stabilize coordination environments not found for the pure oxides or sulfides (e.g., square planar CoO_2 arrays in $Ba_2Cu_2CoO_2S_2$) (1). Most of the oxysulfide compounds prepared thus far contain the early transition metals Ti, V, Nb, Ta. For the titanium oxysulfides, several different structural motifs are encountered. With relatively high oxide concentrations (i.e., O:S > 0.5), three-dimensional structures are found with edge and corner sharing Ti octahedra (cf. $La_6Ti_2S_8O_5$ and $La_4Ti_3S_4O_8$) (9). At lower oxide concentrations (i.e., 0.1 < O:S < 0.2), a novel class of layered phases containing linked $Ti_4O_4S_2$ clusters has been obtained (cf. $La_{8+x}Ti_{8+y}S_{24}O_4$ and $La_{20}Ti_{11}S_{44}O_6$) (4, 5, 7, 8). At very low oxygen concentration, the compound $Ba_6Ti_5S_{15}O$ has been prepared (O:S = 0.07) and shown to adopt a $BaTiS_3$-related structure (11).

A recent study by Palvadeau *et al.* (3) showed that significant amounts of chloride could be incorporated in these types of compounds through the formation of sulfide/chloride solid solutions. Their oxygen-rich compound, $La_5Ti_6S_3Cl_3O_{15}$, was prepared from an LaOCl precursor and showed statistical distributions of S and Cl in the crystal structure. We report here the syntheses and structural details of two new oxychlorosulfides, $Bi_{0.5}La_{13.5}Ti_8S_{29}Cl_4O_4$ and $La_{23.1}Ti_{16.2}S_{49}Cl_8O_8$. The latter is a composite of the $La_{14}Ti_8S_{33}O_4$ and $La_{8+x}Ti_{8+y}S_{24}O_4$ oxysulfide structure types described previously (8). $Bi_{0.5}La_{13.5}Ti_8S_{29}Cl_4O_4$ is isostructural with $La_{14}Ti_8S_{33}O_4$ (7) but is not isomorphic. It has orthorhombic symmetry in contrast to the monoclinic for $La_{14}Ti_8S_{33}O_4$, with bismuth and chlorine partially substituted on some of the lanthanum and sulfur sites, respectively. These new phases reveal the remarkable substitutional and structural flexibility within this class of compounds.

EXPERIMENTAL

A. Synthesis

All reagents were purchased from CERAC and used without further purification. $La_{23.1}Ti_{16.2}S_{49}Cl_8O_8$ was prepared from La_2S_3, TiO_2, Ti and S in a 9:4:14:21 ratio. $LaCl_3$ (30% by weight) was added as a flux. The starting materials were ground in an N_2 dry box and loaded in a carbon-coated silica ampule. The ampule was sealed under vacuum and fired at 950°C for 4 days. The ampule was cooled to 850°C at 3°C/h and then cooled to room temperature in 3 h. The sample was washed with ethanol and filtered to dissolve and remove the $LaCl_3$ flux. The reaction yielded a black crystalline powder with small black single crystals (ca. 0.1 mm on edge, ~5% of sample).

0022-4596/99 $30.00

$Bi_{0.5}La_{13.5}Ti_8S_{29}Cl_4O_4$ was prepared from Bi, La_2S_3, Ti, and S in a 2:2:3:8 ratio. $LaCl_3$ was added as a flux (20% by weight). The starting materials were ground in an N_2 dry box and loaded in a carbon-coated silica ampule. The ampule was sealed under vacuum and fired at 950°C for 5 days. The ampule was cooled to 825°C at 3°C/h and then cooled to room temperature in 3 h. The sample was washed with ethanol and filtered to dissolve and remove the $LaCl_3$ flux. The reaction yielded a black crystalline powder with small black single crystals (ca. 0.1 mm on edge, ~75% of sample).

B. Analysis

Single crystals were analyzed by wavelength-dispersive X-ray analysis (WDS) on a JEOL JXA-840 A electron probe microanalyzer. $LaPO_4$, Ti, Bi, and MoS_2 were used as WDS standards. Crystals from the various reactions were acid washed with HNO_3 (ca. 50%) prior to analysis.

C. Structural Determination

$Bi_{0.5}La_{13.5}Ti_8S_{29}Cl_4O_4$. A black irregular block with dimensions $0.20 \times 0.10 \times 0.10\ mm^3$ was placed on the Enraf-Nonius CAD-4 diffractometer. The crystal's final cell parameters and crystal orientation matrix were determined from 25 reflections in the range $17.45 < \theta < 17.63°$. The cell constants were confirmed with axial photographs. Data were collected [Mo$K\alpha$] with $\omega/2\theta$ scans over the range $2.65 < \theta < 25.00°$ with a scan width of $(0.60 + 0.48 \tan\theta)°$ and a variable scan speed of 1.2–1.5° min^{-1} with each scan recorded in 96 steps with the outermost 16 steps on each end of the scan being used for background measurement. Six standard reflections were monitored at 30-min intervals of X-ray exposure with minimal variations in intensity being observed; data were not corrected. Seven Ψ-scan reflections were collected over the range $8.0 < \theta < 16.2°$; the absorption correction was applied with transmission factors ranging from 0.0096–0.0307. Data were corrected for Lorentz and polarization factors and reduced to F_0^2 and $\sigma(F_0^2)$ using the program XCAD4 (12). The SHELXTL (13) program package was used to determine the orthorhombic space group possibilities, to apply the absorption correction, and to set up the initial files. Systematic absences indicated one of three possible space groups: the centrosymmetric space group *Cmcm* (No. 63), the noncentrosymmetric space group $Cmc2_1$ (No. 36), or the noncentrosymmetric space group *Ama*2 (No. 40). Intensity statistics favored the centric space group *Cmcm*. The structure was determined by direct methods, using the program XS (14), with the successful location of many lanthanum and titanium atoms. The remaining atoms were found from a series of difference-Fourier least squares cycles and the structure refined with XL (15). Three of the La sites were found to be composed of both La and Bi. Refinement was conducted using EXYZ and EADP (15) instructions to sort out the relative occupancies of each on the individual sites. The R(1) and R(3) sites were found to have La:Bi ratios of 0.922:0.078 and 0.469:0.031, respectively. The R(5) site had a La:Bi ratio of 0.847:0.016. La(6) was 13.7% occupied. All sulfur and chlorine atoms were refined as sulfur due to our inability to differentiate between the two by X-ray diffraction. All atoms were refined anisotropically during the final series of cycles and to convergence [$\Delta/\sigma \le 0.001$] with $R(F) = 4.17\%$, $wR(F^2) = 8.80\%$ and GOF = 1.096 for all 2352 unique reflections. A final difference-Fourier map was essentially featureless with the largest peak ($|\Delta\rho|$) = 1.85 $eÅ^{-3}$) being greater than 2.5 Å from the nearest atom. This peak was found to be spurious, after inclusion and further refinements, and was removed from further consideration.

$La_{23.1}Ti_{16.2}S_{49}Cl_8O_8$. A shiny black block-shaped crystal with dimensions $0.120 \times 0.175 \times 0.150\ mm^3$ was placed on the Enraf-Nonius CAD-4 diffractometer. The crystal's final cell parameters and crystal orientation matrix were determined from 25 reflections in the range $17.6 < \theta < 18.2°$. The final cell parameters were confirmed with DIRAX (16) and CREDUC (17). Data were collected [Mo$K\alpha$] with $\omega/2\theta$ scans over the range $2.0 < \theta < 25.0°$ as described above. Minimal variations in intensity were observed and the data were not corrected for decay. Nine Ψ-scan reflections were collected over the range $7.1 < \theta < 17.0°$ resulting in a max:min transmission correction of 0.1217:0.0578. Data were processed as described above.

Systematic absences indicated the monoclinic centrosymmetric space group $C2/m$ (No. 12) or the noncentrosymmetric space groups $C2$ (No. 5) or Cm (No. 8). Intensity statistics favored the centrosymmetric possibility, $C2/m$. Successful solution and refinement of the structure confirmed this choice. The programs XS (14) and XL (15) were used to solve and refine the structure, based upon F_0^2 and $\sigma(F_0^2)$. The remaining atoms were located from refinement–difference-Fourier map cycles. As refinement converged it became apparent that two sites were composites, being composed of both La and Ti atoms in varying occupancy. The $M(6)$ site contained La and Ti with a final ratio of 0.918:0.082, respectively. The second site, the $M(7)$ site, possesses multiple disorder with three clearly apparent atom sites, La(7)/Ti(7a)/Ti(7b), all within close proximity to one another and also to themselves thereby reducing the maximum overall occupancy of either of these latter two atoms to 0.50. After careful analysis and extensive refinement, the final occupancy for the La(7):Ti(7a):Ti(7b) site was found to be 0.05336:0.11031:0.08634 with an overall site occupancy of 0.25. Atom S(18) was also found to lie approximately 0.880 Å from itself and input at half occupancy. Ti(8) was also partially occupied with occupancy of 0.06974 where full site occupancy would be 0.25. All atoms, except for the La(7)/Ti(7a)/Ti(7b) and O(2) sites, were

refined anisotropically. All sulfur and chlorine atoms were refined as sulfur due to our inability to differentiate between the two by X-ray diffraction. The structure was refined to convergence [$\Delta/\sigma \leq 0.001$] with $R(F) = 4.94\%$, $wR(F^2) = 12.00\%$, and GOF = 1.081 for all 3952 unique reflections. A final difference-Fourier map was essentially featureless with the largest peak ($|\Delta\rho| = 2.5$ eÅ^{-3}) within 1 Å of a lanthanum atom.

RESULTS

A. Synthesis and Characterization

The compounds $Bi_{0.5}La_{13.5}Ti_8S_{29}Cl_4O_4$ and $La_{23.1}Ti_{16.2}S_{49}Cl_8O_8$ were prepared from the elements and binaries (oxides and sulfides) at 950°C with use of $LaCl_3$ as a flux. The compounds were characterized by single-crystal X-ray diffraction, powder X-ray diffraction (XRD), energy-dispersive X-ray analysis (EDX), and wavelength dispersive X-ray analysis (WDS).

The XRD profile for the $La_{23.1}Ti_{16.2}S_{49}Cl_8O_8$ reaction mixture showed TiS_2 to be the major phase. WDS analysis of acid washed $La_{23.1}Ti_{16.2}S_{49}Cl_8O_8$ single crystals gave the following atomic ratios: La/Ti = 1.3, (S + Cl)/La = 2.3, (S + Cl)/Ti = 3.0, S/La = 2.0, S/Ti = 2.6, S/Cl = 6.4. The ratios from the X-ray analysis are La/Ti = 1.4, (S + Cl)/La = 2.5, and (S + Cl)/Ti = 3.5. Accounting for the errors associated with the WDS experiment, we assign the formula of the compound as $La_{23.1}Ti_{16.2}S_{49(\pm 2)}Cl_{8(\pm 2)}O_8$ which has an average Ti oxidation state of +3.3.

The XRD profile for the $Bi_{0.5}La_{13.5}Ti_8S_{29}Cl_4O_4$ reaction mixture showed essentially single phase $La_6Ti_5S_{16}$, a $(LaS)_{1+x}TiS_2$ type compound (18–20). WDS analysis gave the following atomic ratios: La/Ti = 1.4, La/Bi = 28, Ti/Bi = 19, (S + Cl)/La = 2.4, (S + Cl)/Ti = 3.4, S/La = 2.1, S/Ti = 3.0, S/Cl = 7.4. The ratios from the X-ray analysis are La/Ti = 1.7, La/Bi = 27, Ti/Bi = 16, (S + Cl)/La = 2.4, and (S + Cl)/Ti = 4.1. Accounting for the errors associated with the WDS experiment, we assign the formula of the compound as $Bi_{0.5(\pm 0.2)}La_{13.5(\pm 0.2)}Ti_8S_{29(\pm 1)}Cl_{4(\pm 1)}O_4$, which has an average Ti oxidation state of +3.5. In both compounds, the Ti content determined from WDS analysis is high, which may be due to a problem with the Ti standard. In the X-ray refinement of $Bi_{0.5}La_{13.5}Ti_8S_{29}Cl_4O_4$, the free refinement of the Bi occupancy gave a total content of $Bi_{0.35}$ which was fixed to $Bi_{0.50}$ based on the WDS analysis. Aside from these two issues, the agreement between WDS and X-ray is good.

B. General Solid State Structures

Both compounds contain substantial amounts of chloride that form a solid solution with the sulfide ions. Because of the similarities in atomic scattering and ionic radii, we were not able to differentiate between sulfide and chloride in either structure. To simplify the structural analysis, only sulfur was used in the X-ray refinement though all sites are potentially S/Cl mixtures. For brevity, mixed S/Cl sites are identified by a Q in the formulas that follow.

$Bi_{0.5}La_{13.5}Ti_8S_{29}Cl_4O_4$ is orthorhombic, space group *Cmcm*, and a summary of the crystallographic data is given in Table 1. Bond distances for $Bi_{0.5}La_{13.5}Ti_8S_{29}Cl_4O_4$ are given in Table 2. $Bi_{0.5}La_{13.5}Ti_8S_{29}Cl_4O_4$ is isostructural with $La_{14}Ti_8S_{33}O_4$ (7) and contains $^2_\infty[(Ti_4Q_2O_4)(TiQ_6)_{4/2}]$ oxysulfide layers that alternately stack with $[La_6Ti_2Q_{19}]$ layers along the *c*-axis (see Fig. 1). The major difference between the two compounds is that $Bi_{0.5}La_{13.5}Ti_8S_{29}Cl_4O_4$ has orthorhombic symmetry, whereas $La_{14}Ti_8S_{33}O_4$ is monoclinic. We assume that the change in symmetry is associated with the substitutions of Bi for La and/or Cl for S in the structure.

$La_{23.1}Ti_{16.2}S_{49}Cl_8O_8$ is monoclinic, space group *C*2/*m*. A summary of the crystallographic data is given in Table 1. The bond distances for $La_{23.1}Ti_{16.2}S_{49}Cl_8O_8$ are given in Table 3. $La_{23.1}Ti_{16.2}S_{49}Cl_8O_8$ has $[La_{4.1}Ti_{4.9}Q_{20}]$ (A) and $[La_6Ti_{2.19}Q_{19}]$ (B) layers that alternately stack with the $^2_\infty[(Ti_4Q_2O_4)(TiQ_6)_{4/2}]$ (OS) oxysulfide layers along the *c*-axis following the sequence: $\cdots$A–OS–B–OS–A–OS–B$\cdots$ (see Fig. 2). $La_{23.1}Ti_{16.2}S_{49}Cl_8O_8$ is a composite of the two types of oxysulfides described previously. The $[La_6Ti_{2.19}Q_{19}]$ layer B is isostructural with the $[La_6Ti_2S_{19}]^{12-}$ layer in $La_{14}Ti_8S_{33}O_4$ (7) and the $[La_{4.1}Ti_{4.9}Q_{20}]$ layer A is

TABLE 1
Summary of Crystallographic Data for $Bi_{0.5}La_{13.5}Ti_8S_{29}Cl_4O_4$ and $La_{23.1}Ti_{16.2}S_{49}Cl_8O_8$

Formula	$Bi_{0.5}La_{13.5}Ti_8S_{29}Cl_4O_4$	$La_{23.1}Ti_{16.2}S_{49}Cl_8O_8$
Formula weight (amu)	3479.42	5968.9
Space group	*Cmcm*	*C*2/*m*
a (Å)	14.7463(9)	14.8278(4)
b (Å)	14.9009(8)	14.7241(3)
c (Å)	22.680(4)	20.2724(6)
B (°)	90	103.541(3)
V (Å^3)	4983.5(10)	4303.0(2)
T (K)	153(2)	153(2)
Z	4	2
ρ_{cal} (g/cm^3)	4.645	4.586
No. of refln.	4704	15465
No. of unique refln.	2352	3952
No. of unique refln. with $F_0 > 4\sigma F_0$	1992	3547
No. of variables	174	275
Radiation [Mo$K\alpha$] (Å)	0.71073	0.71073
μ (mm^{-1})	15.641	13.998
*R*1 [all data] %[a]	4.17	4.94
*R*1 [$F_0 > 4\sigma F_0$] %[a]	3.32	4.46
*wR*2 [$F_0 > 4\sigma F_0$] %[a]	8.36	11.61
GOF	1.090	1.081

Note. [a] $R1 = [\sum(F_0 - F_c)/\sum(F_0)]$ and $wR_2 = [\sum wF_0^2 - F_c^2)/\sum(F_0^2)]^{1/2}$.

TABLE 2
Selected Bond Distances and Angles for $Bi_{0.5}La_{13.5}Ti_8S_{29}Cl_4O_4$[a,b]

Bond	Distance
R(1)–S/Cl(9)	2.851(2)
R(1)–S/Cl(8)	2.964(2)
R(1)–S/Cl(5)	2.986(2)
R(1)–S/Cl(7)	3.002(2)
R(1)–S/Cl(12)	3.025(2)
R(1)–S/Cl(3)	3.0713(6)
R(1)–S/Cl(4)	3.087(2)
R(1)–S/Cl(1)	3.159(2)
La(2)–O(1)	2.523(7)
La(2)–S/Cl(11)	2.808(4)
La(2)–S/Cl(7)	2.959(2)
La(2)–S/Cl(5)	2.961(2)
La(2)–S/Cl(3)	3.124(3)
La(2)–S/Cl(4)	3.146(2)
R(3)–O(2)	2.526(7)
R(3)–S/Cl(8)	2.999(2)
R(3)–S/Cl(12)	3.005(2)
R(3)–S/Cl(1)	3.050(2)
R(3)–S/Cl(3)	3.079(3)
R(3)–S/Cl(6)	3.164(3)
La(4)–S/Cl(11)	2.786(4)
La(4)–S/Cl(9)	2.826(3)
La(4)–S/Cl(11)	2.887(4)
La(4)–S/Cl(6)	2.896(3)
La(4)–S/Cl(5)	3.024(2)
La(4)–S/Cl(10)	3.378(5)
La(4)–S/Cl(2)	3.600(3)
R(5)–S/Cl(9)	2.845(3)
R(5)–S/Cl(10)	2.932(5)
R(5)–S/Cl(6)	2.9597(11)
R(5)–S/Cl(8)	3.021(2)
R(5)–S/Cl(8)′	3.058(2)
R(5)–S/Cl(1)	3.136(2)
R(5)–S/Cl(5)	3.152(3)
R(5)–S/Cl(5)	3.461(3)
La(6)–S/Cl(5)	2.540(7)
La(6)–S/Cl(9)	2.672(7)
La(6)–S/Cl(10)	2.716(8)
La(6)–S/Cl(9)	2.832(7)
La(6)–S/Cl(1)	3.072(7)
La(6)–S/Cl(8)	3.325(7)
La(6)–S/Cl(8)′	3.520(7)
La(6)–S/Cl(6)	3.543(7)
Ti(1)–S/Cl(12)	2.419(4)
Ti(1)–S/Cl(4)	2.459(3)
Ti(1)–S/Cl(1)	2.472(3)
Ti(1)–S/Cl(7)	2.472(4)
Ti(2)–S/Cl(3)	2.290(4)
Ti(2)–S/Cl(8)	2.426(3)
Ti(2)–S/Cl(6)	2.519(4)
Ti(2)–S/Cl(5)	2.577(3)
Ti(3)–O(1)	1.952(8)
Ti(3)–O(3)	1.962(8)
Ti(3)–S/Cl(4)	2.322(2)
Ti(3)–S/Cl(2)	2.638(2)
Ti(3)–Ti(3)	2.997(4)
Ti(3)–Ti(4)	2.998(3)
Ti(4)–O(3)	1.949(8)
Ti(4)–O(2)	1.955(8)
Ti(4)–S/Cl(1)	2.376(2)
Ti(4)–S/Cl(1)	2.376(2)
Ti(4)–S/Cl(2)	2.588(3)
Ti(4)–Ti(4)′	2.948(4)
Ti(4)–Ti(3)	2.998(3)

[a] All M–S/Cl distances listed in this table are potentially M–(S/Cl) composite distances.
[b] R(1) is 92.2% La and 7.8% Bi; R(3) is 46.9% La and 3.1% Bi; R(5) is 84.7% La and 1.6% Bi; La(6) is 13.7% occupied.

isostructural with the disordered sulfide layer in the infinitely adaptive series $La_{8+x}Ti_{8+y}S_{24}O_4$, where $(x + y) \leq 2$ (8).

C. The Common $^2_\infty[(Ti_4Q_2O_4)(TiQ_6)_{4/2}\}^{(12+\delta)-}$ Layers

$Bi_{0.5}La_{13.5}Ti_8S_{29}Cl_4O_4$ and $La_{23.1}Ti_{16.2}S_{49}Cl_8O_8$ both contain $^2_\infty[(Ti_4Q_2O_4)(TiQ_6)_{4/2}]^{(12+\delta)-}$ oxysulfide layers that are essentially identical to the oxysulfide layers in $La_{14}Ti_8S_{33}O_4$ and $La_{8+x}Ti_{8+y}S_{24}O_4$ and related compounds (4, 7, 8). A projection of this layer viewed down the c-axis of $Bi_{0.5}La_{13.5}Ti_8S_{29}Cl_4O_4$ is given in Fig. 3a. The $Ti_4Q_2O_4$ clusters in $Bi_{0.5}La_{13.5}Ti_8S_{29}Cl_4O_4$ are bisected by mirror planes running parallel to the b-axis. The Ti(3) and Ti(4) atoms in the $Ti_4Q_2O_4$ clusters are not crystallographically equivalent but are in virtually identical environments. The Ti–O distances, 1.95(1) Å (ave), and Ti–Q distances 2.35(3) (ave), 2.62(3) Å (ave), are similar to the Ti–S distances in the oxysulfides described previously. The $Ti_4Q_2O_4$ clusters are linked in the a–b plane via edge shared Ti(1)Q_6 octahedra with average Ti–Q distances of 2.46(3) Å. In $Bi_{0.5}La_{13.5}Ti_8S_{29}Cl_4O_4$, there is a 4.78 Å shift between successive $^2_\infty[(Ti_4Q_2O_4)(TiQ_6)_{4/2}]$ layers in the b-direction (see Fig. 1).

The $^2_\infty[(Ti_4Q_2O_4)(TiQ_6)_{4/2}]$ layer of $La_{23.1}Ti_{16.2}S_{49}Cl_8O_8$ (Fig. 3b) is virtually identical to that of $Bi_{0.5}La_{13.5}Ti_8Cl_4O_4$ except that the mirror plane is parallel to the a-axis and bisects two crystallographically distinct titanium atoms, Ti(2) and Ti(4), with Ti–O and Ti–Q distances identical to those in $Bi_{0.5}La_{13.5}Ti_8S_{29}Cl_4O_4$ within experimental error. There is a 4.70-Å shift between successive $^2_\infty[(Ti_4Q_2O_4)(TiQ_6)_{4/2}]$ sheets separating the $[La_6Ti_{2.19}Q_{19}]$ (B) layers in the a-direction in $La_{23.1}Ti_{16.2}S_{49}Cl_8O_8$. In contrast, there is no shift between successive $^2_\infty[(Ti_4Q_2O_4)(TiQ_6)_{4/2}]$ layers separating $[La_{4.1}Ti_{4.9}Q_{20}]$ (A) layers.

D. The $[La_6Ti_2Q_{19}]$ Layer in $Bi_{0.5}La_{13.5}Ti_8S_{29}Cl_4O_4$

In $Bi_{0.5}La_{13.5}Ti_8S_{29}Cl_4O_4$, the $^2_\infty[(Ti_4Q_2O_4)(TiQ_6)_{4/2}]$ layers are separated by two isolated Ti(2)Q_6 octahedra that

TABLE 3
Bond Distances (Å) for $La_{23.1}Ti_{16.2}S_{49}Cl_8O_8$[a,b]

Bond	Distance
La(1)–O(2)	2.517(9)
La(1)–S/Cl(16)	2.832(5)
La(1)–S/Cl(3)	2.976(2)
La(1)–S/Cl(7)	3.077(2)
La(2)–O(1)	2.513(6)
La(2)–S/Cl(15)	2.824(3)
La(2)–S/Cl(2)	2.991(2)
La(2)–S/Cl(3)	3.013(2)
La(2)–S/Cl(4)	3.0829(6)
La(2)–S/Cl(6	3.084(2)
La(2)–S/Cl(7)	3.093(2)
La(2)–S/Cl(9)	3.115(2)
La(3)–O(3)	2.524(9)
La(3)–S/Cl(16)	2.821(5)
La(3)–S/Cl(2)	3.011(2)
La(3)–S/Cl(6)	3.090(2)
La(3)–S/Cl(9)	3.103(3)
La(3)–S/Cl(4)	3.106(3)
La(4)–O(2)	2.484(9)
La(4)–S/Cl(12)	3.017(2)
La(4)–S/Cl(3)	3.022(2)
La(4)–S/Cl(8)	3.051(2)
La(4)–S/Cl(17)	3.061(3)
La(4)–S/Cl(10)	3.151(3)
La(5)–O(3)	2.475(9)
La(5)–S/Cl(18)	2.819(5)
La(5)–S/Cl(2)	2.947(2)
La(5)–S/Cl(11)	3.002(3)
La(5)–S/Cl(17)	3.110(3)
La(5)–S/Cl(5)	3.128(2)
M(6)–M(6)′	0.952(5)
M(6)–S/Cl(6)	2.644(3)
M(6)–S/Cl(7)	2.649(3)
M(6)–S/Cl(9)	2.770(4)
M(6)–S/Cl(6)	3.185(3)
M(6)–S/Cl(7)′	3.191(3)
M(6)–S/Cl(16)	3.449(3)
M(6)–S/Cl(15)	3.474(3)
La(7)–Ti(7B)	0.792(14)
La(7)–Ti(7A)	0.820(10)
La(7)–S/Cl(15)	2.510(5)
La(7)–S/Cl(16)	2.520(5)
La(7)–S/Cl(13)	2.725(3)
La(7)–S/Cl(13)	2.725(3)
La(7)–S/Cl(7)	4.280(2)
La(7)–S/Cl(6)	4.281(2)
Ti(7A)–Ti(7B)	1.140(13)
Ti(7A)–S/Cl(16)	1.700(12)
Ti(7A)–S/Cl(15)	2.640(6)
Ti(7A)––S/Cl(13)	2.836(11)
Ti(7A)–S/Cl(16)′	3.340(12)
Ti(7A)–S/Cl(7)	3.849(8)
Ti(7A)–S/Cl(6)	3.858(9)
Ti(7B)–S/Cl(15)	1.717(15)
Ti(7B)–S/Cl(16)	2.642(6)
Ti(7B)–S/Cl(13)	2.838(5)
Ti(7B)–S/Cl(15)′	3.302(15)
Ti(7B)–S/Cl(6)	3.868(7)
Ti(7B)–S/Cl(7)	3.868(7)

TABLE 3—*Continued*

Bond	Distance
La(8)–S/Cl(14)	2.850(3)
La(8)–S/Cl(19)	2.941(5)
La(8)–S/Cl(10)	2.9622(8)
La(8)–S/Cl(12)	2.970(2)
La(8)–S/Cl(12)	3.051(2)
La(8)–S/Cl(8)	3.053(2)
La(8)–S/Cl(11)	3.127(3)
La(8)–S/Cl(11)	3.475(3)
La(9)–O(1)	2.469(6)
La(9)–S/Cl(14)	2.852(3)
La(9)–S/Cl(12)	2.980(2)
La(9)–S/Cl(3)	3.004(2)
La(9)–S/Cl(11)	3.012(3)
La(9)–S/Cl(2)	3.014(2)
La(9)–S/Cl(17)	3.0748(6)
La(9)–S/Cl(5)	3.075(2)
La(9)–S/Cl(8)	3.151(2)
La(10)–S/Cl(18)	2.776(5)
La(10)–S/Cl(14)	2.811(3)
La(10)–S/Cl(18)	2.870(5)
La(10)–S/Cl(10)	2.887(3)
La(10)–S/Cl(11)	3.063(3)
La(10)–S/Cl(19)	3.341(5)
La(10)–S/Cl(1)	3.467(4)
Ti(1)–S/Cl(4)	2.311(3)
Ti(1)–S/Cl(9)	2.495(3)
Ti(2)–O(3)	1.965(6)
Ti(2)–O(1)	1.969(7)
Ti(2)–S/Cl(5)	2.325(3)
Ti(2)–S/Cl(6)	2.349(3)
Ti(2)–S/Cl(13)	2.630(3)
Ti(2)–S/Cl(1)	2.637(3)
Ti(2)–Ti(2)′	3.023(3)
Ti(2)–Ti(4)′	3.024(2)
Ti(2)–Ti(3)	3.087(2)
Ti(3)–S/Cl(3)	2.438(3)
Ti(3)–S/Cl(8)	2.464(3)
Ti(3)–S/Cl(7)	2.465(3)
Ti(3)–S/Cl(2)	2.465(3)
Ti(3)–S/Cl(5)	2.473(3)
Ti(3)–S/Cl(6)	2.474(3)
Ti(3)–Ti(4)	3.098(2)
Ti(4)–O(2)	1.964(6)
Ti(4)–O(1)	1.965(7)
Ti(4)–S/Cl(7)	2.361(3)
Ti(4)–S/Cl(8)	2.370(3)
Ti(4)–S/Cl(13)	2.595(3)
Ti(4)–S/Cl(1)	2.630(3)
Ti(4)–Ti(4)′	2.988(3)
Ti(5)–S/Cl(17)	2.271(4)
Ti(5)–S/Cl(12)	2.480(3)
Ti(5)–S/Cl(11)	2.509(3)
Ti(5)–S/Cl(10)	2.567(4)
Ti(5)–Ti(8)	2.805(3)
Ti(8)–S/Cl(10)	2.514(3)
Ti(8)–S/Cl(12)	2.532(2)

[a] All *M*–S/Cl distances listed in this table are potentially *M*–(S/Cl) composite distances.

[b] *M*(6) is 46% La and 4% Ti. The ratio La(7):Ti(7a):Ti(7b) is 0.05336: 0.11031:0.08634. Ti(8) is 28% occupied.

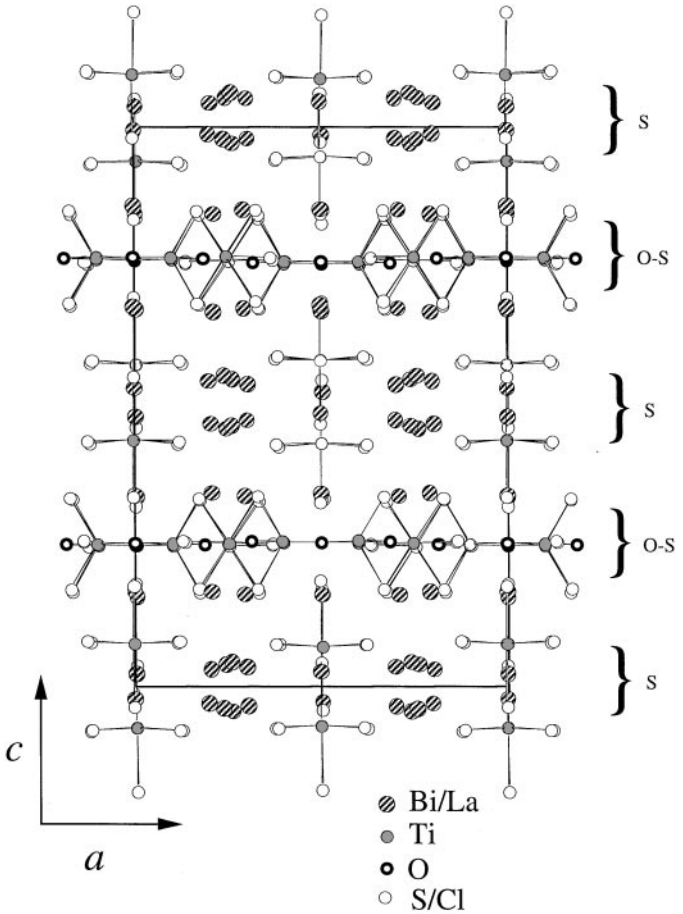

FIG. 1. An (0 1 0) projection of the $Bi_{0.5}La_{13.5}Ti_8S_{29}Cl_4O_4$ structure. The heavy lines represent the unit cell. The $^2_\infty[(Ti_4Q_2O_4)(TiQ_6)_{4/2}]$ oxysulfide layers (O–S) and $[La_6Ti_2Q_{19}]$ layers (S) are labeled on the drawing. The bonds to Bi and La have been omitted for clarity.

are interlinked with four La(5)Q_8 square antiprisms and two La(4)Q_9 tricapped trigonal prisms in the a–b plane. This layer has the composition $[La_6Ti_2Q_{19}]$ (omitting the S/Cl atoms shared with the $^2_\infty[(Ti_4Q_2O_4)(TiQ_6)_2]^{-12}$ layers) and is shown in Fig. 4a. Eight additional La^{3+} ions fill the nine-coordinate holes between the two types of layers forming $LaOQ_8$ tricapped trigonal prisms. These sites are almost identical to the La(1), La(2), and La(3) sites in $La_{14}Ti_8S_{33}O_4$ (7). In $Bi_{0.5}La_{13.5}Ti_8S_{29}Cl_4O_4$, however, the La(1) and La(3) sites (designated R(1) and R(3)), form a La/Bi solid solution with La : Bi ratios of 0.922 : 0.078 and 0.469 : 0.031, respectively.

The Ti(2)Q_6 octahedron is highly distorted with Ti–Q distances ranging from 2.290(4) Å to 2.577(3) Å (see Table 2). The Ti(2)Q_6 octahedron shares a common face with the La(4)Q_9 tricapped trigonal prism and a common face with the La(5)Q_9 polyhedron. The La(4)–Q contacts are in the range 2.786(4)–3.378(5) Å. A longer 10th contact to Q(2) is observed at 3.600(3). La(5) forms a solid solution with bismuth and is disordered over a second site with La(6) which is 0.638(6) Å away. The La(5), Bi(5), and La(6) occupancies were constrained to sum to 1.0, which gave refined occupancies of 0.847 : 0.016 : 0.137, respectively. La(5)–Q distances are in the range 2.845(3)–3.461(3) Å, whereas La(6) is eight coordinate with La–Q contacts in the range 2.540(7)–3.543(7) Å. Q(11) is disordered over two sites that are 50% occupied and 0.821(9) Å apart. The same disorder at the S(11) site is also observed in $La_{14}Ti_8S_{33}O_4$ (7) and $La_{23.1}Ti_{16.2}S_{49}Cl_8O_8$ (see Q(18) below) but the disorder of La(5) and La(6) is absent.

E. The $[La_6Ti_{2.28}Q_{19}]$ Layer in $La_{23.1}Ti_{16.2}S_{49}Cl_8O_8$

One of the layers separating the $^2_\infty[(Ti_4Q_2O_4)(TiQ_6)_{4/2}]$ network in $La_{23.1}Ti_{16.2}S_{49}Cl_8O_8$ is a $[La_6Ti_{2.28}Q_{19}]$ layer that is very similar to the $[La_6Ti_2Q_{19}]$ sheets in $La_{14}Ti_8S_{33}O_4$ (7) and $Bi_{0.5}La_{13.5}Ti_8S_{29}Cl_4O_4$ (Fig. 4b). In $La_{14}Ti_8S_{33}O_4$ and $Bi_{0.5}$ $La_{13.5}Ti_8S_{29}Cl_4O_4$, there are isolated Ti(2)Q_6 octahedra, whereas $La_{23.1}Ti_{16.2}S_{49}Cl_8O_8$ has a $[Ti_{2.28}Q_{12}]$ "trimer" (see Fig. 4c). The $[Ti_{2.28}Q_{12}]$ trimers are interlinked with four La(10)Q_8 square antiprisms and two La(8)Q_9 tricapped trigonal prisms in the a–b plane. In addition, the La(8) sites are fully occupied and not

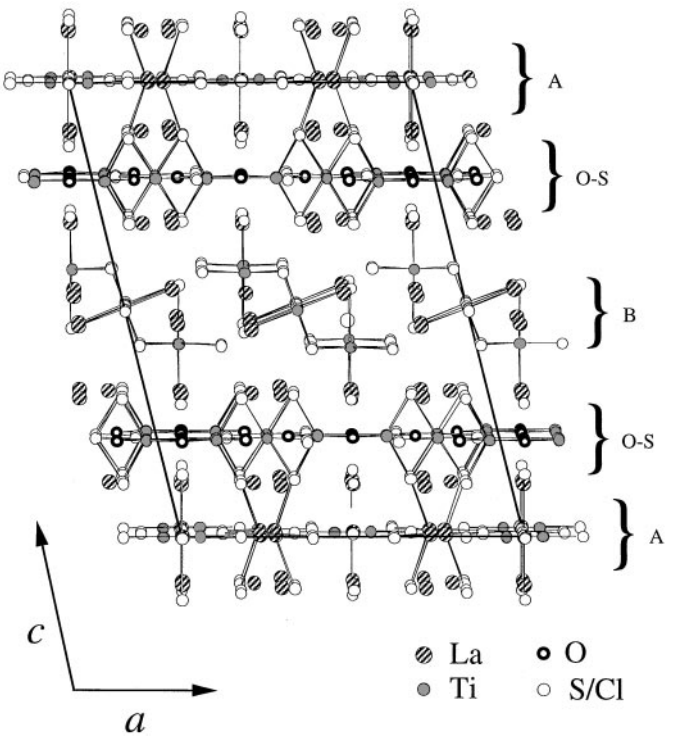

FIG. 2. An (0 1 0) projection of the $La_{23.1}Ti_{16.2}S_{49}Cl_8O_8$ structure. The heavy lines represent the unit cell. The $^2_\infty[(Ti_4Q_2O_4)(TiQ_6)_{4/2}]$ oxysulfide layers (O–S), $[La_{4.1}Ti_{4.9}Q_{20}]$ (A) and $[La_6Ti_{2.19}Q_{19}]$ (B) layers are labeled on the drawing. The bonds to La are omitted for clarity.

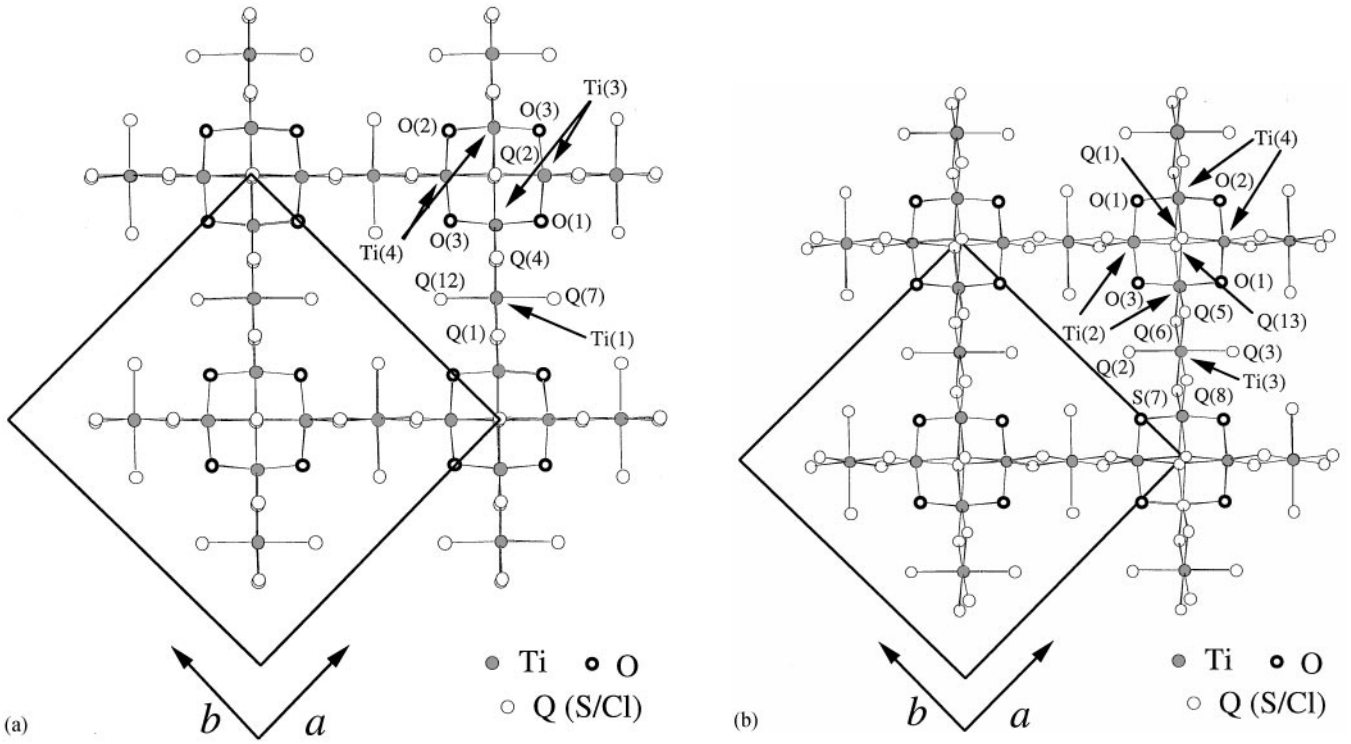

FIG. 3. (0 0 1) projections of the $^{2}_{\infty}[(Ti_4Q_2O_4)(TiQ_6)_{4/2}]$ oxysulfide layers in (a) $Bi_{0.5}La_{13.5}Ti_8S_{29}Cl_4O_4$ and (b) $La_{23.1}Ti_{16.2}S_{49}Cl_8O_8$. The box represents the unit cell. The symbol Q denotes an S/Cl composite.

disordered in contrast to the La(5) and La(6) sites in $Bi_{0.5}La_{13.5}Ti_8S_{29}Cl_4O_4$.

The $[Ti_{2.28}Q_{12}]$ "trimer" contains two crystallographically distinct titanium atoms, Ti(5) and Ti(8), in a face-shared trioctahedron with Ti–Ti separations of 2.805(3) Å. The Ti(5)–Q(17) distance is short at 2.271(4) Å, whereas the other Ti–Q distances are normal. The corresponding Ti–Q bonds in $La_{14}Ti_8S_{33}O_4$ and $Bi_{0.5}La_{13.5}Ti_8S_{29}Cl_4O_4$ are also short at 2.258(5) Å and 2.290(4) Å, respectively. Ti(8) is 28% occupied in $La_{23.1}Ti_{16.2}S_{49}Cl_8O_6$ but the corresponding sites in $La_{14}Ti_8S_{33}O_4$ and $Bi_{0.5}La_{13.5}Ti_8S_{29}Cl_4O_4$ are vacant. Although there is clearly not enough electron density at this site to be a fully occupied titanium atom, the atomic distances are typical of octahedral Ti–S contacts. Q(18) is disordered over two sites that are 50% occupied and 0.89(1) Å apart (cf. Q(11) in $Bi_{0.5}La_{13.5}Ti_8S_{29}Cl_4O_4$).

F. The $[La_{4.1}Ti_{4.9}Q_{20}]$ Layer in $La_{23.1}S_{49}Cl_8O_8$

The other layer separating the $^{2}_{\infty}[(Ti_4Q_2O_4)(TiQ_6)_{4/2}]$ layers in $La_{23.1}Ti_{16.2}S_{49}Cl_8O_8$ is a $[La_{4.1}Ti_{4.9}Q_{20}]$ layer which is isostructural with the disordered sulfide sheets in the infinitely adaptive series $La_{8+x}Ti_{8+y}S_{24}O_4$, where $(x + y) \leq 2$ (8). This layer contains three distinct polyhedral sites; a Ti(1)Q_6 octahedron, one $M(7)Q_6$ octahedron and two $M(6)Q_6$ octahedra (see Fig. 5), where M is a combination of La and Ti. The central Ti(1)Q_6 octahedron shares its four corners in the a–b plane with four $M(6)Q_6$ octahedra to form a two-dimensional square net. Each neighboring octahedron is rotated by 45° about the Ti(1)–Q(4)–M(6) vector. The $M(6)Q_6$ octahedra share common edges with the Ti(3)Q_6 octahedra in the $^{2}_{\infty}[(Ti_4Q_2O_4)(TiQ_6)_{4/2}]$ layers to form rutile-like edge-sharing chains that run parallel to the c-axis. The $M(7)Q_6$ octahedra fill the holes in the square net and link the $Ti_4Q_2O_4$ clusters from adjacent oxysulfide layers along the c-axis.

The M(7) "site" is disordered over five positions and contains variable amounts of La and Ti. The $La_{1-x}Ti_xQ_6$ octahedron contains two Q(15) and two Q(16) atoms in the a–b plane and two Q(13) atoms along the c-axis. The M(7) site in $La_{23.1}Ti_{16.2}S_{49}Cl_8O_8$ displays the same fourfold symmetry as the M(2) site in the tetragonal $La_{8+x}Ti_{8+y}S_{24}O_4$ series (8); however, in this compound it is generated by two crystallographically independent positions. One titanium, Ti(7A), resides on a mirror plane and generates a site ~1.6 Å from itself via a twofold rotation axis and the other titanium Ti(7B) resides on the twofold rotation axis and generates a site ~1.6 Å from itself through mirror plane. The fourfold disorder is quite regular (see Fig. 5), but the fourfold symmetry is not cyrstallographically imposed as it

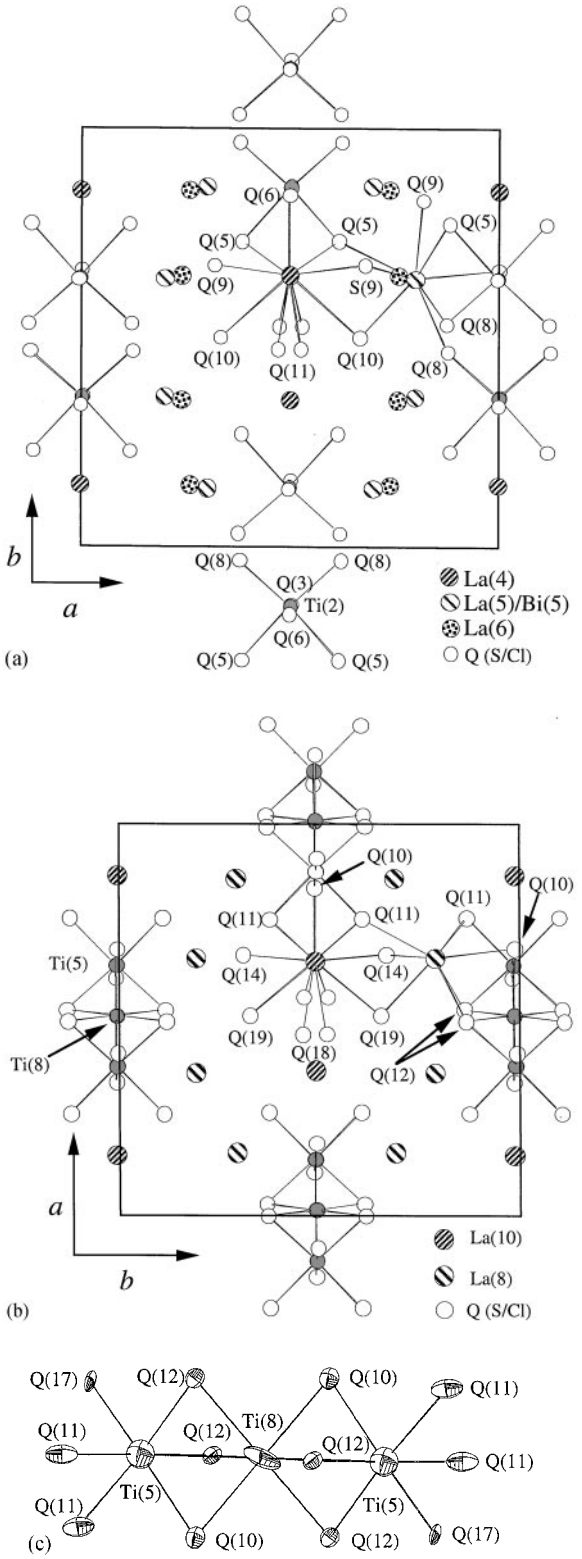

FIG. 4. (001) Projections of (a) the $[La_6Ti_2Q_{19}]$ layer in $Bi_{0.5}La_{13.5}Ti_8S_{29}Cl_4O_4$ and (b) the $[La_6Ti_{2.19}Q_{19}]$ layer in $La_{23.1}Ti_{16.2}S_{49}Cl_8O_8$. For clarity, only the La–S bonds to two of the polyhedra are shown. (c) An ORTEP drawing of the partially occupied Ti_3Q_{12} in $La_{23.1}Ti_{16.2}S_{49}Cl_8O_8$. The symbol Q denotes an S/Cl composite.

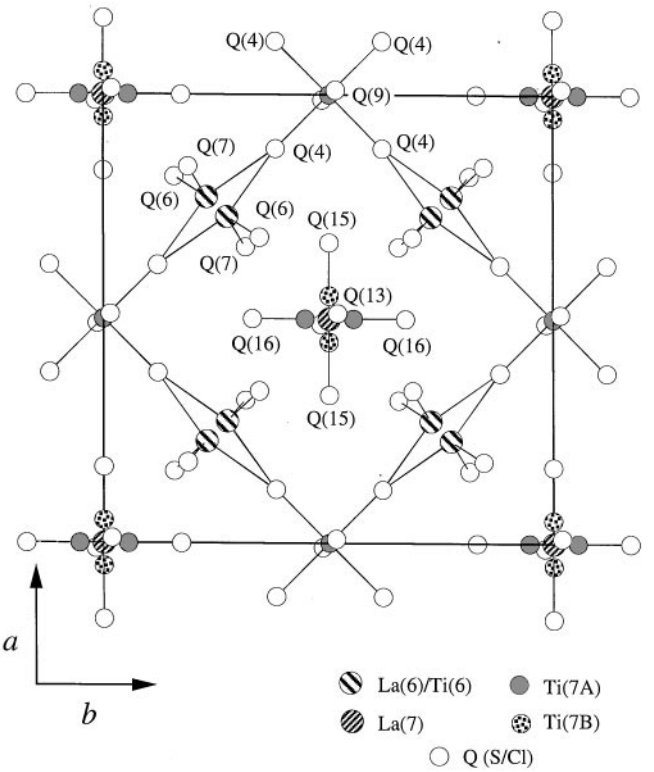

FIG. 5. An (001) projection of the $[La_{4.1}Ti_{4.9}Q_{20}]$ layer in $La_{23.1}Ti_{16.2}S_{49}Cl_8O_8$. The symbol Q denotes an S/Cl composite.

was in the $La_{8+x}Ti_{8+y}S_{24}O_4$ series (8). The amount of lanthanum and titanium on the $M(7)$ site was refined such that the total occupancy of the octahedron was 100%. The refined ratios of La(7):Ti(7A):Ti(7B) are 0.21:0.44:0.35. Due to the five different metal atom positions at the $M(7)$ site, the $Q(15)$ and $Q(16)$ positions represent an average or "composite" of the five different polyhedra present; four TiQ_5 square pyramids and one LaQ_6 octahedron. This composite character is virtually identical to that in the $La_{8+x}Ti_{8+y}S_{24}$ O_4 series (8). Due to the composite character and the S/Cl solid solution formation, distances to $Q(15)$ and $Q(16)$ are not meaningful in determining accurate M–S separations. A discussion of the bonding anomalies and coordination geometries that result from the complex composite nature of this site can be found in Ref. (8) and need not be repeated here.

DISCUSSION

$Bi_{0.5}La_{13.5}Ti_8S_{29}Cl_4O_4$ and $La_{23.1}Ti_{16.2}S_{49}Cl_8O_8$ are two new members of the $Ti_4S_2O_4$ compounds that possess common $^2_\infty[(Ti_4Q_2O_4)(TiS_6)_{4/2}]^{(12+\delta)-}$ oxysulfide layers (7, 8). The O:(S + Cl) ratios in these compounds (0.14 and 0.12, respectively) are in the range of all other compounds with this structural motif. More importantly, these

compounds show that extensive solid solution formation can be accomodated on several sites. Three substitutionally active sites illustrated in this study are Cl-for-S substitution, Bi-for-La substitution, and Ti-for-vacancy substitution (the Ti(8) site in $La_{23.1}Ti_{16.2}S_{49}Cl_8O_8$). Previous studies have shown that unusual La-for-Ti substitution occurs on two sites in the $La_{8+x}Ti_{8+y}S_{24}O_4$ series (8) and is evident in the $M(6)$ and $M(7)$ sites in $La_{23.1}Ti_{16.2}S_{49}Cl_8O_8$ as well. In addition, the La(7), Ti(7a), Ti(7b) disorder is virtually identical to that in the $La_{1+x}Ti_{1+y}S_{24}O_4$ compounds; however, the fourfold disorder in $La_{23.1}Ti_{16.2}S_{49}Cl_8O_8$ is not crystallographically imposed due to the low $C2/m$ crystal symmetry. This finding indicates that the unusual disorder and odd coordination geometries are not an artifact of the tetragonal symmetry of the $La_{1+x}Ti_{1+y}S_{24}O_4$ phases (8).

Although the site of Bi substitution is clearly evident from the structural analysis due to the large difference in scattering of La and Bi, the site of Cl substitution was not obvious. We believe that the chloride substitutions are predominately not in the oxysulfide layers in that most of the subtle structural differences observed in the present compounds occur in the interleaving layers. Both compounds also have mixed valent titanium and it is unclear if the Ti^{3+} is localized or delocalized throughout the structure.

$Bi_{0.5}La_{13.5}Ti_8S_{29}Cl_4O_4$ is isostructural with $La_{14}Ti_8S_{33}O_4$; however, the former has orthorhombic $Cmcm$ symmetry, whereas the latter is monoclinic $C2/m$. $La_{14}Ti_8S_{33}O_4$ is clearly monoclinic, and cannot be transformed up to an orthorhombic system. Since $Bi_{0.5}La_{13.5}Ti_8S_{29}Cl_4O_4$ and $La_{14}Ti_8S_{33}O_4$ had almost identical heating processes, it may be the presence of the bismuth or chloride that affects the change in symmetry. Even though $Bi_{0.5}La_{13.5}Ti_8S_{29}Cl_4O_4$ and $La_{14}Ti_8S_{33}O_4$ have different crystal symmetries, the atomic distances to each of the equivalent sites are virtually identical. These trends are not surprising considering the similarities in ionic radii of lanthanum and bismuth (VIII coord. La^{3+}, $r_i = 1.30$ Å; VIII coord. Bi^{3+}, $r_i = 1.31$ Å) (21). The one notable difference between the two is the presence of the La(5)/La(6) disorder in $Bi_{0.5}La_{13.5}Ti_8S_{29}Cl_4O_4$ which is not observed in $La_{14}Ti_8S_{33}O_4$. Despite this difference, the Ti–(S/Cl) and La–(S/Cl) distances are identical in $La_{14}Ti_8S_{33}O_4$ and $Bi_{0.5}La_{13.5}Ti_8S_{29}Cl_4O_4$. Once again, the incorporation of Cl has little or no effect on the M–(S/Cl) distance due to the similarities in ionic radii (VI coordinate S^{2-}, $r_i = 1.84$ Å; VI coordinate Cl^-, $r_i = 1.81$ Å) (21).

$La_{23.1}Ti_{16.2}S_{49}Cl_8O_8$ is quite interesting due to the fact that it is a composite of the two general types of oxysulfides previously reported (7, 8). The $[La_{4.1}Ti_{4.9}S_{20}]$ layer in $La_{23.1}Ti_{16.2}S_{49}Cl_8O_8$ is isostructural with the disordered sulfide layer in the infinitely adaptive series $La_{8+x}Ti_{8+y}S_{24}O_4$, where $(x + y) \leq 2$ and the $[Sr_{2.2}Ti_{1.8}S_{10}]$ layer in $Sr_{5.8}La_{4.4}Ti_{7.8}S_{24}O_4$. The $[La_6Ti_{2.19}Q_{19}]$ layer in $La_{23.1}Ti_{16.2}S_{49}Cl_8O_8$ is virtually isostructural to the $[La_6Ti_2Q_{19}]$ layers in $La_{14}Ti_8S_{33}O_4$ and $Bi_{0.5}La_{13.5}Ti_8S_{29}Cl_4O_4$.

ACKNOWLEDGMENTS

We thank the NSF-DMR-9223060 for financial support of this work. We thank Mr. Scott Sirchio for the WDS data.

REFERENCES

1. W. J. Zhu, P. H. Hor, A. J. Jacobson, G. Crisci, T. A. Albright, S.-H. Wang, and T. Vogt, *J. Am. Chem. Soc.* **119,** 12,398 (1997).
2. W. Zhu and P. H. Hor, *J. Solid State Chem.* **130,** 319 (1997).
3. P. Palvadeau, M.-C. Boyer, A. Meerschaut, and J. Rouxel, *J. Solid State Chem.* **139,** 220 (1998).
4. L. Cario, C. Deudon, A. Meerschaut, and J. Rouxel, *J. Solid State Chem.* **136,** 46 (1998).
5. C. Deudon, A. Meerschaut, L. Cario, and J. Rouxel, *J. Solid State Chem.* **120,** 164 (1995).
6. J. M. Mayer, L. F. Schneemeyer, T. Siegrist, J. V. Waszczk, and B. V. Dover, *Angew. Chem. Int. Ed. Engl.* **31,** 1645 (1993).
7. L. J. Tranchitella, J. C. Fettinger, and B. W. Eichhorn, *Chem. Mater.* **8,** 2265 (1996).
8. L. J. Tranchitella, J. C. Fettinger, S. F. Heller-Zeisler, and B. W. Eichhorn, *Chem. Mater.* **10,** 2078 (1998).
9. J. A. Cody and J. A. Ibers, *J. Solid State Chem.* **114,** 406 (1995).
10. T. D. Brennan and J. A. Ibers, *J. Solid State Chem.* **98,** 82 (1992).
11. A. C. Sutorik and M. G. Kanatzidis, *Chem. Mater.* **10,** 1700 (1994).
12. K. Harms, XCAD4. Program for the Lp-correction of Nonius CAD-4 diffractometer data. University of Marburg, Germany, 1993.
13. G. M. Sheldrick, SHELXTL, Version 5.03. Siemens Analytical X-ray Instruments Inc. Madison, WI, 1994.
14. G. M. Sheldrick, *Acta Crystallogr. A* **46,** 467 (1990).
15. G. M. Sheldrick, Shelxl93, Program for the refinement of crystal structures. University of Göttingen, Germany, 1993.
16. A. J. M. Duisenberg, *J. Appl Crystallogr.* **25,** 92 (1992).
17. E. J. Gabe, Y. L. Page, J.-P. Charland, F. L. Lee, and P. S. White, *J. Appl. Crystallogr.* **22,** 384 (1989).
18. P. C. Donohue, *J. Solid State Chem.* **12,** 80 (1975).
19. A. Meerschaut (Ed.), "Incommensurate Sandwiched Layered Compounds," Trans. Tech., Zurich, 1992.
20. G. A. Wiegers, *Prog. Solid State Chem.* **24,** 1 (1997).
21. R. D. Shannon, *Acta Crystallogr. A* **32,** 751 (1976).